

# Impurity effect as a probe for order parameter symmetry in iron-based superconductors

Tao Zhou,<sup>1</sup> Xiang Hu,<sup>1</sup> Jian-Xin Zhu,<sup>2</sup> and C. S. Ting<sup>1</sup>

<sup>1</sup>Texas Center for Superconductivity and Department of Physics, University of Houston, Houston, Texas 77204

<sup>2</sup>Theoretical Division, Los Alamos National Laboratory, Los Alamos, New Mexico 87545

E-mail: tzhou2@uh.edu

## Abstract.

The pointlike impurity scattering is studied for a superconductor with different pairing symmetries based on a minimal two band model proposed by S. Raghu *et al.* [Phys. Rev. B **77**, R220503 (2008)], and the self-consistent Bogoliubov-de Gennes equations. Two intra-gap resonance peaks are found at or near the nonmagnetic impurity site for a typical  $s_{x^2-y^2}$  symmetry and strong scattering potentials. Such intra-gap resonance peaks are absent for the sign unchanged  $s$ -wave and  $d_{x^2-y^2}$ -wave order parameter. Thus we propose that a non-magnetic impurity with strong scattering potentials can be used to probe the pairing symmetry in iron-based superconductors.

PACS numbers: 71.10.Fd, 74.20.-z

## 1. Introduction

The new family of superconducting materials which contain Fe-As layers has attracted much attention since their discovery [1]. The Fe-As layers are believed to be the conducting planes. The band calculations have shown that the Fermi surface includes two hole pockets centered at  $\Gamma$  points and two electron pockets centered at  $M$  points, respectively [2, 3, 4], which is confirmed by angle-resolved photoemission spectroscopy (ARPES) experiments [5, 6, 7, 8, 9, 10]. A number of experiments have indicated that this family of materials is not conventional [11]. Therefore, probing the pairing symmetry is one of the most important issues since it can provide us the information of the pairing mechanism.

So far, the pairing symmetry in iron-based superconductors is still controversial. One popular proposal for the pairing symmetry is the  $s_{\pm}$ -wave gap [12, 13, 14, 15, 16, 17], namely, the superconducting gap is extended  $s$ -wave and has opposite sign for the hole and electron pockets. Experimentally, the  $s$ -wave gap symmetry is supported by penetration depth measurement [18], ARPES [6, 7, 8, 9, 10] and specific heat measurement [19]. In particular, the gap magnitudes at different Fermi surface pockets measured by ARPES experiments agree well with  $s_{x^2y^2} = \cos k_x \cos k_y$  form (here  $k_x$  and  $k_y$  represent the momentum in the unfolded Brillouin zone) [8]. However, although ARPES experiment is a powerful tool to measure the gap magnitude directly, it cannot determine the phase of the superconducting order parameter. Detecting the phase of order parameter is an essential and important step to map out the gap symmetry. Recently several theoretical works propose different ways to measure the sign change of the gap [20, 21, 22, 23, 24]. While for multiband materials, probing the phase of the order parameter is still a quite challenging task.

The impurity effect has been an important part in the studies of the superconductivity [25]. The effect of the impurity scattering is sensitive on the symmetry of the order parameter, thus it is a useful tool to probe the pairing symmetry. A well-known result of  $d$ -wave pairing in the cuprates is the zero bias peak in the local density of states (LDOS) near the non-magnetic impurity site. For the case of iron-based materials, it was proposed that the impurity scattering should be sensitive to the sign change of the  $s_{\pm}$ -symmetry order parameter [17]. Furthermore, the averaged effect of an ensemble of impurities on the thermodynamic properties has been studied in iron-based materials [26, 27, 28, 29, 30]. The impurity-induced intra-gap state forms due to the inter-band scattering [29] for the sign-reversing fully gapped order parameter symmetry. We note that the calculation in Ref [29] is based on a phenomenological approach, namely, they treat the intra-band scattering and inter-band scattering intensity as input parameters and consider an impurity concentration. However, such intra-gap state is not observed in scanning tunneling microscopy (STM) experiments [31, 32, 33, 34]. In fact, the impurity-induced intra-gap states are expected to exist only at or near the impurity site. To study the possibility and property of such states one effective method is to put one or several pointlike impurities in real space and calculate the LDOS at or near the impurity site. Basically two methods can be used, namely, the analytic  $T$ -matrix approach and the self-consistent Bogoliubov-de Gennes (BdG) equations. Based on the first method and taking into account the  $s_{\pm}$  symmetry phenomenologically, very recently Ref. [35] calculated the LDOS near the

impurity site and do find the sharp resonance peaks inside the gap. The peaks will disappear if the phase of the order parameter is taken to be the same. The intra-gap bound states are actually located at the positive and negative energies and the LDOS tends to be zero at low energies. The impurity effect is expected to be sensitive to the detailed band structure [25]. The sensitivity maybe more remarkable for the multi-band materials. Since the calculation in Ref. [35] is based on a band structure which artificially fits the ARPES experiments [36, 37], in the present paper we wish to examine the LDOS at and near the impurity site based on a different two-band model as proposed by Raghu *et al.* [38], and the self-consistent BdG equations. The advantage of the BdG technique is that it calculates the order parameter in a fully self-consistent way. The gap magnitude is expected to be suppressed at and near the impurity site. It is proposed that such suppression effect needs to be taken into account to study the local impurity states [39], i.e., the suppression effect would enhance the intensity of the bound states and the peak width and position also depend on the amplitude of the suppression. For the case of the  $s_{x^2-y^2}$  pairing symmetry, our numerical results show that the intra-gap states exist as long as the scattering potential is strong enough, but the detailed spectra of the local impurity states are quite different and sensitive to the parameters for obtaining the band structure. For a nonmagnetic impurity with positive scattering potential, we obtain two intra-gap resonance peaks. The resonance peaks are located near the coherent peaks for weak potentials and move to lower energy as the potential increases. The weight of the resonance peak with positive energy becomes very pronounced as the scattering potential reaching the unitary limit. For the cases of negative scattering potentials, the intra-gap resonance peaks are moving away from the coherent peaks and are closer to the Fermi energy. The position of the resonance peaks are robust and depend weakly on the scattering potentials. All other features remain practically the same. We also studied the LDOS spectra for the cases of the sign unchanged  $s$ -wave and nodal  $d_{x^2-y^2}$ -wave and no intra-gap peaks are observed. Experimentally the LDOS can be measured by STM experiments, and thus is a useful tool to probe the pairing symmetry of this family of compounds.

The paper is organized as follows. In Sec. II, we introduce the model and work out the formalism. In Sec. III, we present the numerical calculations and discuss the obtained results. Finally, we give a brief summary in Sec. IV.

## 2. Model and formalism

As we mentioned above, iron-based superconducting materials have a layered structure. In the FeAs layer there are two Fe ions per unit cell by taking into account As ions located above or below the Fe-Fe plane. Currently no consensus has been reached on what is the suitable model to capture the essential physics [38, 40, 41, 42, 43, 44, 45, 46]. Some groups argue all five  $3d$  orbitals have to be considered to construct a minimal model [41, 42]. On the other hand, the band calculations have also shown that the main features of the bands that determine the Fermi surface are the two orbitals  $d_{xz}$  and  $d_{yz}$  [47, 48]. Thus the two band model is proposed by several groups [38, 45, 46]. Because we are concerned with the low energy physics in the present work, we expect that the qualitative result does not depend on the detailed band

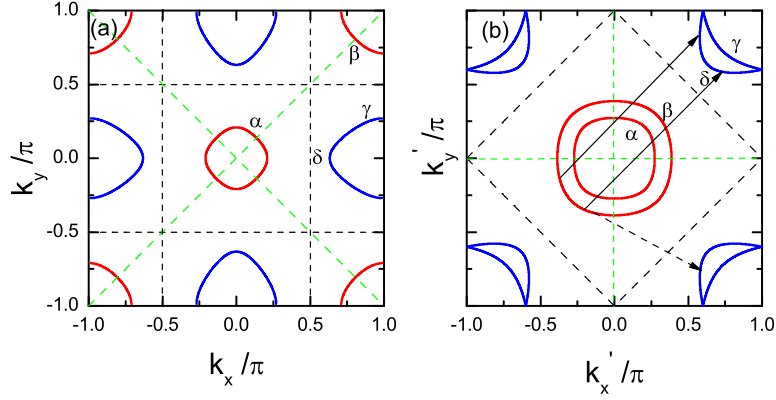


**Figure 1.** The Fermi surface in the extended Brillouin zone and folded Brillouin zone respectively. The black and green dashed lines are nodal lines for  $s_{x^2-y^2}$ -wave, and  $d_{x^2-y^2}$ -wave pairing symmetry, respectively. The red and blue colors represent the hole and electron pockets, respectively.

structure. We here use the two band model considering the two degenerate orbitals  $d_{xz}$  and  $d_{yz}$  per site [38]. On the two-dimensional square lattice, the model Hamiltonian reads,

$$H = H_t + H_\Delta + H_{imp}, \quad (1)$$

where  $H_t$  is the hopping term,

$$H_t = - \sum_{i\mu j\nu\sigma} (t_{i\mu j\nu} c_{i\mu\sigma}^\dagger c_{j\nu\sigma} + h.c.) - t_0 \sum_{i\mu\sigma} c_{i\mu\sigma}^\dagger c_{i\mu\sigma}. \quad (2)$$

where  $i, j$  are the site indices and  $\mu, \nu = 1, 2$  are the orbital indices.  $t_0$  is the chemical potential.

$H_\Delta$  is the pairing term,

$$H_\Delta = \sum_{i\mu j\nu\sigma} (\Delta_{i\mu j\nu} c_{i\mu\sigma}^\dagger c_{j\nu\sigma}^\dagger + h.c.). \quad (3)$$

$H_{imp}$  is the impurity term, which is expressed by,

$$H_{imp} = \sum_{i_m\mu\nu\sigma} V_{s\mu\nu} c_{i_m\mu\sigma}^\dagger c_{i_m\nu\sigma}, \quad (4)$$

where  $i_m$  represents for the impurity site and  $V_{s\mu\nu}$  is the scattering potential.

The Hamiltonian can be diagonalized by solving the BdG equations self-consistently,

$$\sum_j \sum_\nu \begin{pmatrix} H_{i\mu j\nu} & \Delta_{i\mu j\nu} \\ \Delta_{i\mu j\nu}^* & -H_{i\mu j\nu}^* \end{pmatrix} \begin{pmatrix} u_{j\nu\sigma}^n \\ v_{j\nu\bar{\sigma}}^n \end{pmatrix} = E_n \begin{pmatrix} u_{i\mu\sigma}^n \\ v_{i\mu\bar{\sigma}}^n \end{pmatrix}, \quad (5)$$

where the Hamiltonian  $H_{i\mu j\nu}$  is expressed by,

$$H_{i\mu j\nu} = -t_{i\mu j\nu} + (V_s \delta_{i,i_m} - t_0) \delta_{ij} \delta_{\mu\nu}. \quad (6)$$

The superconducting order parameter and the local electron density  $n_{i\mu}$  satisfy the following self-consistent conditions,

$$\Delta_{i\mu j\nu} = \frac{V_{i\mu j\nu}}{4} \sum_n (u_{i\mu\uparrow}^n v_{j\nu\downarrow}^{n*} + u_{j\nu\uparrow}^n v_{i\mu\downarrow}^{n*}) \tanh\left(\frac{E_n}{2K_B T}\right), \quad (7)$$

$$n_{i\mu} = \sum_n |u_{i\mu\uparrow}^n|^2 f(E_n) + \sum_n |v_{i\mu\downarrow}^n|^2 [1 - f(E_n)]. \quad (8)$$

Here  $V_{i\mu j\nu}$  is the pairing strength and  $f(x)$  is the Fermi distribution function.

The LDOS is expressed by,

$$\rho_i(\omega) = \sum_{n\mu} [|u_{i\mu\sigma}^n|^2 \delta(E_n - \omega) + |v_{i\mu\bar{\sigma}}^n|^2 \delta(E_n + \omega)], \quad (9)$$

where the delta function  $\delta(x)$  is taken as  $\Gamma/\pi(x^2 + \Gamma^2)$ , with  $\Gamma = 0.004$ . The supercell technical is used to calculate the LDOS.

In the following calculation, we use the hopping constant suggested by Ref. [38], where  $t_{1-3}$  are hopping constants between the same orbital, expressed by,

$$t_{i1, i\pm\hat{x}1} = t_{i2, i\pm\hat{y}2} = t_1 = -1.0, \quad (10)$$

$$t_{i2, i\pm\hat{x}2} = t_{i1, i\pm\hat{y}1} = t_2 = 1.3, \quad (11)$$

$$t_{i\mu, i\pm\hat{x}\pm\hat{y}\mu} = t_3 = -0.85 \quad (\mu = 1, 2). \quad (12)$$

$t_4$  is the inter-orbital hopping constant, expressed by,

$$t_{i\mu, i\pm(\hat{x}\pm\hat{y})\nu} = t_4 = 0.85 \quad (\mu \neq \nu), \quad (13)$$

$$t_{i\mu, i\pm(\hat{x}-\hat{y})\nu} = -t_4 = -0.85 \quad (\mu \neq \nu). \quad (14)$$

$t_0$  is determined by the doping density. Throughout the work, the energy is measured in units of  $|t_1| = 1$ . The Fermi surface with filling electron density 2.1 per site is plotted in Fig. 1(a). Alternatively, if we consider one unit cell containing two Fe ions, the Fermi surface in the reduced Brillouin zone is plotted in Fig. 1(b).

The pairing symmetry is determined by the pairing potential  $V_{i\mu j\nu}$ . We have carried out extensive calculations to search for favorable pairing symmetry. To summarize, the on-site potential, the nearest-neighbor (NN) potential, and the next-nearest-neighbor (NNN) potential, will produce isotropic  $s$ -wave ( $\Delta = \Delta_0$ ),  $d_{x^2-y^2}$ -wave [ $\Delta = 2\Delta_0(\cos k_x - \cos k_y)$ ], and  $s_{x^2y^2}$ -wave ( $\Delta = 4\Delta_0 \cos k_x \cos k_y$ ) pairing symmetry, respectively. In the present work, we will focus on the characteristic of  $s_{\pm}$  symmetry. We consider the pairing between the same orbital of the NNN site. Without the impurity, self-consistent calculation verified that this kind of pairing produces  $s$ -wave gap symmetry, i.e.,  $\Delta_{i\mu, i\pm\hat{x}\pm\hat{y}\mu} \equiv \Delta_0$ . Transforming the Hamiltonian to the momentum space and diagonalizing the  $4 \times 4$  Hamiltonian, it is easy to verify that the pairing symmetry is exactly the same with the  $s_{x^2y^2}$ -symmetry proposed by Ref. [49], namely, the gap function in the extended Brillouin zone has  $\cos k_x \cos k_y$  form, and has the form of  $\cos k'_x + \cos k'_y$  in the reduced Brillouin zone. The nodal line of the gap function is shown in Fig. 1.

In the following presented results, we choose the filling electron density  $n = 2.1$  per site (electron doped samples with doping  $\delta = 0.1$ ) and pairing potential  $V = 1.2$ . We consider the case for the intra-orbital scattering, namely,  $V_{s\mu\nu} = V_s \delta_{\mu\nu}$ . The parameters are chosen just for illustration. We have checked numerically that our main results are not sensitive to the parameters. The numerical calculation is performed on  $20 \times 20$  lattice with the periodic boundary conditions. The impurity is put at the site (10, 10). A  $80 \times 80$  supercell is taken to calculate the LDOS.

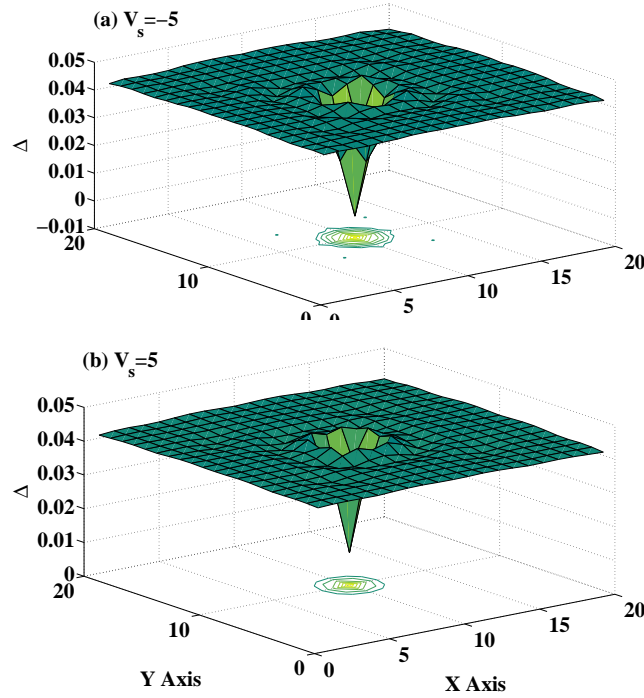


**Figure 2.** Amplitudes of the order parameter in presence of a single nonmagnetic impurity with  $V_s = \mp 5$ .

### 3. Results and discussion

We first illustrate the feature of single nonmagnetic impurity scattering with  $s_{x^2-y^2}$  pairing symmetry. The scattering potential  $V_s$  can be estimated roughly by comparing the energy of the impurity atoms and that of Fe atoms. In real materials, both negative and positive scattering potentials are possible. Thus here we discuss both cases. As it is unclear what an accurate value of the potential strength is, we consider a range of potential values.

We plot the self-consistently determined order parameter amplitudes on the lattice ( $\Delta_i = \frac{1}{8} \sum_{j\mu} \Delta_{i\mu j\mu}$ ) in Fig. 2 for  $V_s = \pm 5$ . As seen, the order parameter is suppressed near the impurity and quite small at the impurity site. It will recover to the uniform value at about  $2 \sim 3$  lattice spacings from the impurity site. Note that the suppression effect is more notable for the negative potential.

The LDOS spectra for different scattering potentials at and near the impurity sites are plotted in Fig. 3. The left panels are the negative potential cases. Obvious impurity states (denoted by the red arrows) exist at the energy about  $\pm 0.57\Delta$  (here  $\Delta$  is the energy of the superconducting coherent peak, denoted by the green arrows). The energy of the impurity resonance peaks depends weakly on the scattering potential  $V_s$ . At the impurity site, for small scattering potential  $V_s$ , two sharp resonance peaks inside the gap are shown, and the resonance peaks are suppressed as  $V_s$  increases and the LDOS tends to zero at the unitary limit. On the other hand, near the impurity site, the intra-gap resonance peaks show up and the intensity increases as the potential  $V_s$  increases. The resonance peaks are remarkable at the NNN site. In the unitary limit, a very sharp and strong resonance peak appears at the positive

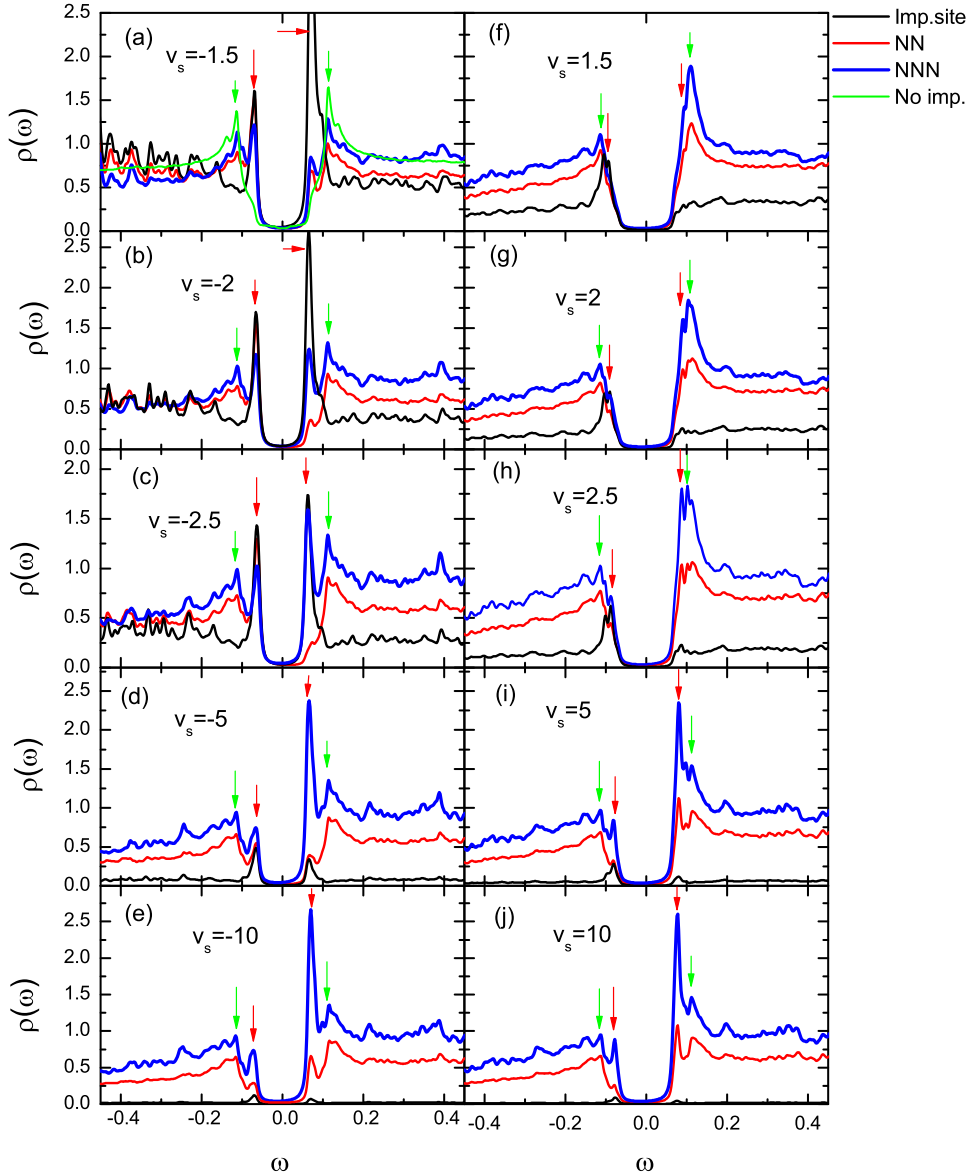


**Figure 3.** The LDOS spectra in presence of a single nonmagnetic impurity for different scattering potentials. The black lines are the LDOS at the impurity site. The red and blue lines are the spectra at NN and NNN sites to the impurity. The left and right panels are for negative and positive scattering potential, respectively. The green line in panel (a) is the density of states spectrum without the impurity. The green and red arrows indicate the superconducting coherent peak and intra-gap resonance peaks, respectively.

energy for the LDOS at the NNN site of the impurity site. This situation may qualitatively correspond to the case for a charged  $\text{Ba}^{+2}$  impurity with a negative or attractive potential seen by electrons on the FeAs layer. This type of impurity may be present in the FeAs layer when  $\text{BaFe}_{2-x}\text{Co}_x\text{As}_2$  is used for STM experiments [50].

The right panels show the effect of a positive scattering potential impurity. We do not see clear resonance peaks at the impurity site for the weak potential, which is different from that of the negative potential. Near the impurity site, similar to the case of the negative potential,

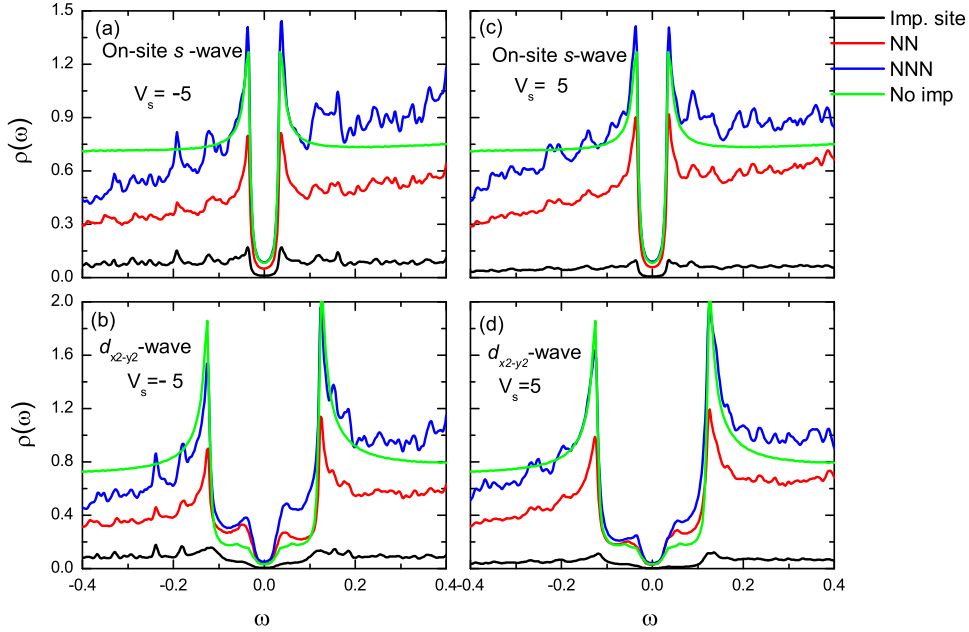


**Figure 4.** The LDOS spectra in presence of a single nonmagnetic impurity for on-site  $s$ -wave symmetry and  $d_{x^2-y^2}$  symmetry with  $V_s = \pm 5$ , respectively. The black lines are the LDOS at the impurity site. The red and blue lines are the spectra at NN and NNN sites to the impurity. The green lines are density of states spectra without the impurity.

the intra-gap resonance peaks show up as the potential increases, while the intensities seem to be smaller than those of the negative potential impurities. The resonance peaks are more remarkable at the NNN site to the impurity, which is similar to that of the negative potential. We also point out that the positions of the two resonance peaks are much closer to the coherent peaks for weak scattering potentials. The intensity of the resonance peaks with positive energy increases and the positions move away from the superconducting coherent peaks to lower energies as the scattering potential increases. For a quite strong impurity scattering potential ( $V_s = 10$ ), the intra-gap peaks are located at the energy about  $\pm 0.7\Delta$ . The spectrum is quite similar to that of the negative potential ( $V_s = -10$ ).

On the whole, we present the LDOS spectra taking into account the impurity scattering for  $s_{x^2y^2}$ -pairing symmetry. The intra-gap states for  $s_{x^2y^2}$ -pairing symmetry obtained here are quite robust for a strong impurity. Experimentally, the intra-gap bound states may be detected by comparing the LDOS spectrum far away the impurity site with that near the impurity site. The intra-gap peaks will show up near the impurity site. We also verified numerically that the main results will not change for many impurities or the impurity scattering potential is not only purely on-site but also extends with a few lattice sites. While for quite weak scattering potentials, the intensity of the intra-gap peaks would decrease and disappear as the potentials are small enough. We have checked that no obvious intra-gap features could be observed as  $|V_s| < 1$ .

We now discuss the impurity scattering effect for different pairing symmetries. The LDOS spectra at and near the impurity site for the sign unchanged  $s$ -wave (on-site pairing)



and  $d_{x^2-y^2}$ -wave (NN pairing) with  $V_s = \pm 5$  are shown in Fig. 4. For the case of the sign unchanged  $s$ -wave pairing symmetry, we can see clearly two superconducting coherent peaks with the energies equal to those of the density of states without the impurity. The intensity of the coherent peaks are suppressed at the impurity site and its NN site. No intra-gap peaks are observed. For the case of the  $d$ -wave pairing symmetry, two intra-gap plateaus can be observed inside the gap. The spectra are significantly different with those of the cuprates. In fact, here the calculations are based on the two-band model. For the  $d_{x^2-y^2}$ -wave order parameter, the hole pockets around the  $\Gamma$  point are nodal and the electron pockets around the  $M$  point are nodeless. As a result, the low energy spectra are mainly contributed by the hole pockets, which lead to the intra-gap plateaus. The interband scattering may enhance the intensity of the plateaus while no intra-gap bound states are observed for  $d_{x^2-y^2}$  symmetry.

On the whole, we present the LDOS spectra taking into account the impurity scattering for different pairing symmetries. The intra-gap states for  $s_{x^2y^2}$ -pairing symmetry obtained here are quite robust for a strong impurity. The electron operator for each orbital is a linear combination of quasiparticle operators from all bands, therefore the four Fermi surface pockets in Fig.1(b) are contributed by the hybridization of the two orbitals. With this observation, one can find out that even the intra-orbital impurity scattering will give rise to the scattering between different bands with the scattering strength weighted by the Bogoliubov amplitude [51]. Comparing the LDOS spectra for the  $s_{x^2y^2}$  pairing symmetry shown in Fig.3 and those for the sign-unchanged  $s$ -wave symmetry shown in Figs. 4(a) and 4(b), we expect that the intra-gap bound state for the  $s_{x^2y^2}$  pairing symmetry is due to sign change of the order parameter between the different Fermi surface pockets. As a result, we propose that this can be used to detect the sign reversal of the order parameter. However, we stress that the sign change of the order parameter is just one of the essential conditions for the bound states but not sufficient. The scattering is weighted by the Bogoliubov amplitude so the band structure and the detailed scattering potential form is also important. For the current model, the  $d$ -wave pairing symmetry will not produce the bound states, as seen in Figs.4(c) and 4(d). We here focus our discussion on the properties of the  $s_{\pm}$  pairing symmetry. The reason for the absence of the bound states for  $d$ -wave pairing symmetry can be investigated further through the momentum space scattering potential based on the  $T$ -matrix method while this issue is not concerned here.

Comparing all the relevant results with different pairing symmetries, we propose that one strong nonmagnetic impurity can be used to probe the pairing symmetry and detect the sign reversal of the order parameter.

#### 4. Summary

In summary, we have studied the point-like single non-magnetic impurity scattering effect in iron-based superconductors based on self-consistent BdG equations. The LDOS at and near the impurity site are calculated and the spectra have their unique features for different pairing symmetry. Especially, for the case of the  $s_{x^2y^2}$ -wave symmetry, two intra-gap peaks show up as the impurity scattering potential is strong enough. This may also be easily detected by the

STM experiments through substituting the Fe atom with a nonmagnetic atoms (e.g., Zn or Ba atoms etc.). As a result, we propose that the non-magnetic impurity can be used to probe the pairing symmetry of iron based superconductors.

*Note added-* After we posted our work in ArXiv, we note that another group also did similar calculations [53] based on BdG equations and T-matrix method using the same two band model proposed by S. Raghu *et al.* Their results are similar to ours.

## acknowledgements

The authors would like to thank S. H. Pan, Ang Li, and Degang Zhang for useful discussions. One of us (X.H.) also acknowledges the hospitality of Los Alamos National Laboratory (LANL), where part of this work was initiated. This work was supported by the Texas Center for Superconductivity at the University of Houston and by the Robert A. Welch Foundation under the Grant no. E-1146 (T.Z., X.H., C.S.T.) and the U.S. DOE at LANL under Contract No. DE-AC52-06NA25396, the U.S. DOE Office of Science, and the LANL LDRD Program (J.X.Z.).

## References

- [1] Kamihara Y *et al.* 2008 *J. Am. Chem. Soc.* **130** 3296
- [2] Singh D J and Du M H 2008 *Phys. Rev. Lett.* **100** 237003
- [3] Ishibashi S, Terakura K, and Hosono H 2008 *J. Phys. Soc. Jpn.* **77** 053709
- [4] Nakamura K, Arita R, and Imada M 2008 *J. Phys. Soc. Jpn.* **77** 093711
- [5] Lu D H *et al.* 2008 *Nature (London)* **455** 81
- [6] Ding H *et al.* 2008 *Europhys. Lett.* **83** 47001
- [7] Kondo T *et al.* 2008 *Phys. Rev. Lett.* **101** 147003
- [8] Nakayama K *et al.* 2009 *Europhys. Lett.* **85** 67002
- [9] Evtushinsky D V *et al.* 2009 *Phys. Rev. B* **79** 054517
- [10] Liu C *et al.* 2008 *Phys. Rev. Lett.* **101** 177005
- [11] For a review, see, e.g., Sadovskii M V 2008 *Phys. Usp.* **51** 1201
- [12] Mazin I I, Singh D J, Johannes M D, and Du M H 2008 *Phys. Rev. Lett.* **101** 057003
- [13] Chubukov A V, Efremov D V, and Eremin I 2008 *Phys. Rev. B* **78**, 134512
- [14] Yao Z-J, Li J-X, and Wang Z D 2009 *New J. Phys.* **11**, 025009
- [15] Yu S-L, Kang J, and Li J-X 2009 *Phys. Rev. B* **79** 064517
- [16] Wang F, Zhai H, Ran Y, Vishwanath A, and Lee D-H 2009 *Phys. Rev. Lett.* **102**, 047005
- [17] Cvetkovic V and Tesanovic Z 2009 *Europhys. Lett.* **85** 37002
- [18] Hashimoto K *et al.* 2009 *Phys. Rev. Lett.* **102** 017002
- [19] Mu G, Luo H, Wang Z, Shan L, Ren C, Wen H-H 2009 *Phys. Rev. B* **79** 174501
- [20] Tsai W-F, Yao D-X, Bernevig B A, Hu J P 2009 *Phys. Rev. B* **80** 012511
- [21] Ghaemi P, Wang F, Vishwanath A 2009 *Phys. Rev. Lett.* **102** 157002
- [22] Parker D and Mazin I 2008 arxiv: 0812.4416.
- [23] Wu J and Phillips P 2009 *Phys. Rev. B* **79** 092502
- [24] Zhang Y-Y, Fang C, Zhou X, Seo K, Tsai W-F, Bernevig B A, and Hu J P 2009 *Phys. Rev. B* **80** 094528
- [25] Balatsky A V, Vekhter I, and Zhu J-X 2006 *Rev. Mod. Phys.* **78** 373
- [26] Chubukov A V, Efremov D V, and Eremin I 2008 *Phys. Rev. B* **78** 134512
- [27] Bang Y, Choi H Y, and Won H 2009 *Phys. Rev. B* **79** 054529
- [28] Parker D, Dolgov O V, Korshunov M M, Golubov A A, and Mazin I I 2008 *Phys. Rev. B* **78** 134524

- [29] Senga Y and Kontani H 2009 *New J. Phys.* **11** 035005
- [30] Vorontsov A B, Vavilov M G, and Chubukov A V 2009 *Phys. Rev. B* **79** 140507(R)
- [31] Millo O, Asulin I, Yuli O, Felner I, Ren Z-A, Shen X-L, Che G-C, and Zhao Z-X 2008 *Phys. Rev. B* **78** 092505
- [32] Boyer M C, Chatterjee K, Wise W D, Chen G F, Luo J L, Wang N L, and Hudson E W 2008 arXiv:0806.4400
- [33] Pan M H, He X B, Li G R, Wendelken J F, Jin R, Sefat A S, McGuire M A, Sales B C, Mandrus D, and Plummer E W 2008 arXiv:0808.0895
- [34] Yin Y, Zech M, Williams T L, Wang X F, Wu G, Chen X H, and Hoffman J E 2009 *Phys. Rev. Lett.* **102** 097002
- [35] Zhang D G 2009 *Phys. Rev. Lett.* **103** 186402
- [36] Sekiba Y *et al.* 2009 *New J. Phys.* **11** 025020
- [37] Terashima K *et al.* 2009 *Proc. Natl. Acad. Sci. U.S.A.* **106** 7330
- [38] Raghu S, Qi X-L, Liu C-X, Scalapino D J, and Zhang S-C 2008 *Phys. Rev. B* **77** 220503(R)
- [39] Shnirman A, Adagideli I, Goldbart P M, and Yazdani A 1999 *Phys. Rev. B* **60** 7517
- [40] Korshunov M M and Eremin I 2008 *Phys. Rev. B* **78** 140509(R)
- [41] Kuroki K, Onari S, Arita R, Usui H, Tanaka Y, Kontani H, and Aoki H 2008 *Phys. Rev. Lett.* **101** 087004
- [42] Nakamura K, Arita R, and Imada M 2008 *J. Phys. Soc. Jpn.* **77** 093711
- [43] Malaeb W *et al.* 2008 *J. Phys. Soc. Jpn.* **77** 093714
- [44] Lee P A and Wen X-G 2008 *Phys. Rev. B* **78** 144517
- [45] Daghofer M, Moreo A, Riera J A, Arrigoni E, Scalapino D J, and Dagotto E 2008 *Phys. Rev. Lett.* **101** 237004
- [46] Moreo A, Daghofer M, Riera J A, and Dagotto E, *Phys. Rev. B* **79**, 134502 (2009)
- [47] Boeri L, Dolgov O V, and Golubov A A 2008 *Phys. Rev. Lett.* **101** 026403
- [48] Vildosola V, Purovskii L, Arita R, Biermann S, and Georges A 2008 *Phys. Rev. B* **78** 064518
- [49] Seo K, Bernevig B A, and Hu J P 2008 *Phys. Rev. Lett.* **101** 206404
- [50] Pan S H *et al.*, private communication
- [51] Graser S, Maier T A, Hirschfeld P J, and Scalapino D J 2009 *New J. Phys.* **11** 025016
- [52] Chubukov A V, Eremin I, and Korshunov M M 2009 *Phys. Rev. B* **79** 220501(R)
- [53] Tsai W-F, Zhang Y-Y, Fang C, and Hu J P 2009 *Phys. Rev. B* **80** 064513